NUMERICAL SIMULATION OF WAVES IN THE NORTH SULAWESI WATERS USING SWAN WAVE MODEL

Yogi Muhammad Andariwan[1,3*], Nining Sari Ningsih[2], Aditya Rakhmat Kartadikaria[1]
[1]Study Program of Magister of Earth Science, Faculty of Earth Sciences and Technology, Bandung Institute of Technology, Bandung 40132, Indonesia.
[2] Research Group of Oceanography, Faculty of Earth Sciences and Technology, Bandung Institute of Technology, Bandung 40132, Indonesia.
[3] Sam Ratulangi Meteorological Station, Indonesian Agency for Meteorological, Climatological and Geophysics.
***** *yogi.andariwan@bmkg.go.id*

Received: August 16, 2024 Reviewed: December 23, 2024 Accepted: January 3, 2025

ABSTRACT

This study investigates wind and wind wave conditions in North Sulawesi waters based on their climatological characteristics and a case study of when high waves occurred during Tropical Cyclone (TC) Kimi. Climatological characteristics are calculated by using ERA5 data and the case study is conducted by simulation using Simulating Waves Nearshore (SWAN) wave model. Model verification was performed by comparing the significant wave height (SWH) from SWAN with observation data from wave buoys in Albatross Bay, Townsville, and Emu Park. The statistical results provide biases of -0.11 m, 0.22 m, and 0.16 m, respectively. The Root Mean Square Error (RMSE) values are 0.14 m, 0.28 m, and 0.23 m, and the correlation coefficients are 0.54, 0.8, and 0.95. During the December- February (DJF) period, wind speed peaks in February (3.0-6.5 m/s), and the SWH reaches 0.5-0.8 m. On 17th of January 2021, Manado's coastline experienced high waves, coinciding with the active phase of TC Kimi near northeastern Australia from 15th to 19th of January 2021. As TC Kimi developed, wind speeds in North Sulawesi increased to 7.0–12 m/s, triggering waves reaching 1.0–1.8 meters with an anomaly of 1–1.5 meters. This wave activity experienced a time lag of +19 hours in response to the wind speeds generated by TC Kimi.

Keywords: SWAN, North Sulawesi, significant wave height, cross correlation, tropical cyclone.

1. Introduction

Around the North Sulawesi waters exists several important atmosphere and ocean phenomenon, such as cyclogenesis [1], variation of mixed layer [2], and Indonesian Throughflow [3]. On the northeast, the western north Pacific (WNP), is location with the highest tropical cyclone activity, where 31% of the global tropical cyclone occurred [4]. For more details, Ningsih et al., 2023 [5] divided the tropical cyclone area around Indonesia into 4 areas, and one of them is western north Pacific. The study discovered between 1979 and 2020, 60.5% of TC occurred in that area. When a TC formed in WNP, the wave heights around the TC can reach 10 m, and in some place, for example in Japan waters, can reach 12 m [6,7]. Waves that generated by TC will spread as a swell and the propagation distance can reach 20,000 km [8]. Some of the swell can reach North Sulawesi waters, especially if the TC trajectory is westward and crosses the Philippines [9].

To understand how climatological condition of a parameter in an area, World Meteorological Organization (WMO), 2018 [10] recommend to observe and calculate the data for 30 years. Wave climate information is very important for various fields, namely sea transportation [5], beach tourism [11] and maritime security [12]. On 17th of January 2021, high waves were observed along the coast of Manado, North Sulawesi, while TC Kimi was active in the waters off northeastern Australia. TC Kimi reached its maximum intensity on 17th of January 2021 with maximum wind speed reached 45 knots (83.3 km/h). Study by Aror et al. [13] found out that high waves in North Sulawesi may influenced by atmospheric disturbance. In addition, previous study by Burrahman, 2021 [14] discovered that the high waves on 17th of January were triggered by meteorological factor and generated high waves with 1.5-2 m height.

This study aims to investigate the influence of TC Kimi on wave conditions in Manado Waters. TC that occurred on DJF period in Australia region can induce positive significant wave height (SWH) anomaly and during DJF period there are 8.53% probability of SWH > 2 m in North Sulawesi [5]. In this study, we will investigate the climatological characteristic and wave condition during TC Kimi by simulating the waves, then calculating the anomaly. Understanding the wave climate in North Sulawesi can provide valuable information for decision-making across various sectors, including tourism, infrastructure development, fisheries, transportation, and maritime security. Additionally, analyzing the

impact of TC Kimi on high waves offers insights into wave occurrences in Manado. This knowledge can help local authorities prepare mitigation strategies to minimize potential damage and fatalities if similar conditions arise in the future.

2. Methods

SWAN model. Delft University of Technology developed SWAN to perform wave simulation in water body with a spatial resolution of less than 25 km [15] and shallow waters [16]. It can be applied to various water bodies, including estuaries [17], straits [18,19], coasts [20,21], gulfs [22], and lakes [23]. Additionally, SWAN is capable of simulating waves in ocean, such as the Northwest Pacific [24] and the Indian Ocean [25], and can even be used for global wave simulations [26].

SWAN is based on the wave action balance equation and incorporates sources and sinks along with complex deep-water process formulations derived from the Wave Modelling (WAM) model, such as wave creation, dissipation, and quadruplet wave-wave interactions [27]. Enhanced formulations for triad wave-wave interactions, bottom friction-induced dissipation, and depth-induced breaking are used to better refine these processes in shallow water. SWAN is a completely spectrum model that takes into consideration all wave orientations and frequencies, which makes it appropriate for modelling how wind waves change along coastlines that are impacted by ambient currents and shallow waters. The following is the expression for the governing equation [28]:

$$\frac{\partial}{\partial t}N + \frac{\partial}{\partial x}c_x N + \frac{\partial}{\partial y}c_y N + \frac{\partial}{\partial \sigma}c_\sigma N + \frac{\partial}{\partial \theta}c_\theta N = \frac{S}{\sigma} \quad (1)$$

with N denotes the action density spectrum (m^2/s). On the left hand, the first component represents the change of action density over time. Propagation throughout the geographic space denoted by second and third component, with velocities c_x and c_y in the x and y directions. The fourth component accounts for frequency shifts due to depth and current variations, with a propagation velocity of c_σ in frequency space. Wave refraction caused by these variations represented by the fifth component, which has propagation velocity c_θ in the directional dimension. All velocity variables are measured in meters per second (m/s). The right hand of the equation is component for source and sink and are described in more detail below,

$$S = S_{in} + S_{nl3} + S_{nl4} + S_{ds,w} + S_{ds,b} + S_{ds,br} \quad (2)$$

with S_{in} is wave generation from wind. Second and third component, S_{nl3} and S_{nl4} are non-linear wave interaction which made up of triad wave and quadruplet wave. Meanwhile fourth to sixth component are for the dissipation of wave energy, with $S_{ds,w}$ is due to white-capping, $S_{ds,b}$ is due to bottom friction and $S_{ds,br}$ is due to wave breaking. All of source and sink terms are in m^2/s^3.

Data. The wind forcing data used in this study is from the European Centre for Medium-Range Weather Forecasts (ECMWF) database. Specifically, we utilized 10-meter wind data from ECMWF Reanalysis v5 (ERA5) [29], which represents the most advanced atmospheric reanalysis dataset available. ERA5 provides hourly wind data with a spatial resolution of 0.25° × 0.25°. Previous studies comparing ERA5 with other wind datasets, such as Climate Forecast System Reanalysis (CFSR), has demonstrated that ERA5 offers superior accuracy and correlation, making it more suitable for wave simulations [30,31,32]. The dataset is available at an hourly temporal resolution and a spatial resolution of 0.5° × 0.5°. For bathymetric data, we employed the General Bathymetric Ocean Chart (GEBCO), which offers a spatial resolution of 15 arc seconds. GEBCO provides integrated elevation data by combining both ocean depth and land topography [33]. However, in wave simulations, SWAN focuses solely on ocean bathymetry. To analyse the wind and wave climate, we utilized monthly averaged wind and wave data from the ERA5, spanning the period from 1974 to 2023. We then computed the monthly averages for the DJF (December-January-February) period, aligning them with the timing of TC Kimi.

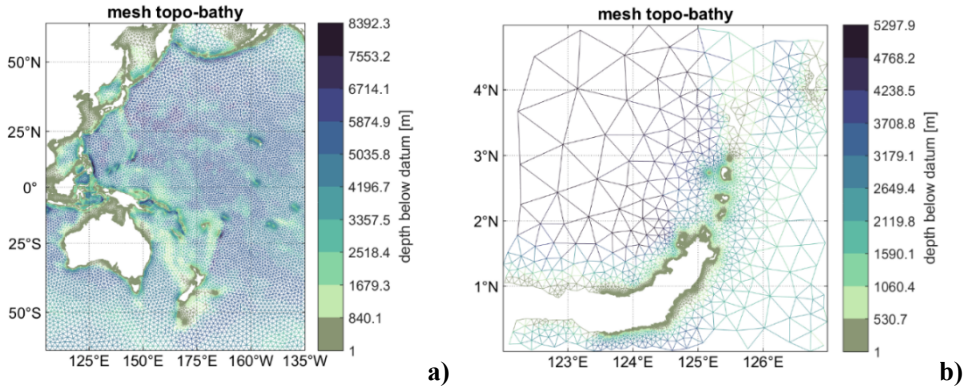

Figure 1. Unstructured grid and bathymetry of (a) model domain and (b) analysis domain.

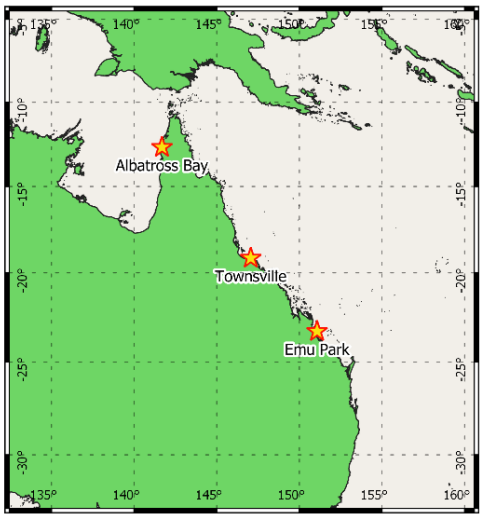

Figure 2. Buoy locations to verify the SWAN output.

Model setup. The global surface wind climate indicates that the strongest wind speeds occur between 30°-60° in both hemispheres [34]. These strong winds generate wind waves, which eventually evolve into swells as they travel away from their source regions. Depending on their height, these swells can propagate over distances ranging from 2,800 to 20,000 km [8]. The first domain which covers a large portion of the Pacific Ocean, enabling the accurate simulation of swells that generated by the trade winds in this ocean. Swells play a crucial role in ocean dynamics and can influence locally generated wind waves. Previous studies have shown that swells originating in the Pacific reach Indonesian waters throughout the year via northeastern passage, such as North Sulawesi and Maluku, except for June-July-August (JJA) [35, 36]. The second domain is the domain for analysis, where the model output is examined. Analysis domain focuses on North Sulawesi located in 0°S–5°N, 122°–127°E. The wave simulation provides hourly outputs with spatial resolution aligned with the model grid.

We used unstructured grid for computational grid. It has several advantages compared the regular nested grid, for example it can create more accurate shoreline, has mesh density variations and can perform simulation in shorter time [20, 37]. To generate the unstructured grid, this study utilizes Oceanmesh2D, a MATLAB-based software to generate grid for ocean modelling [38]. The grid in model domain has 4 km resolution in nearshore and 100 km in off shore. Meanwhile in domain analysis the resolution in nearshore is refined to 100 m. The unstructured grid consisted of 159,653 elements and 93,352 nodes.

To verify SWAN output (Fig. 2), we used wave buoy data provided by Queensland Government in three locations, namely Albatross Bay (141.685° E, 12.688° S), Townsville (147.059° E, 19.159° S) and Emu Park (151.07° E, 23.305° S). Data from the wave buoys are available from 9th of January to 22nd, 2021, and with the temporal resolution of 30-minutes.

To evaluate the accuracy of the model output, we used bias, root mean square error (RMSE), and correlation coefficients (r) for verification.

$$\text{bias (x,y)} = \frac{1}{M}\sum_{i=1}^{M} \Delta H(x,y,t) \quad (3)$$

$$\text{RMSE (x,y)} = \sqrt{\frac{1}{M}\sum_{i=1}^{M}[\Delta H(x,y,t)]^2} \quad (4)$$

$$\text{r (x,y)} = \frac{\sum_{i=1}^{M}[H_m(x,y,t) - \overline{H_m}(x,y,t)][H_o(x,y,t) - \overline{H_o}(x,y,t)]}{\sqrt{\sum_{i=1}^{M}[H_m(x,y,t) - \overline{H_m}(x,y,t)]^2 [H_o(x,y,t) - \overline{H_o}(x,y,t)]^2}} \quad (5)$$

where H_m represents the SWH output from SWAN, while H_o denotes the observation data. $\overline{H_m}$ and $\overline{H_o}$ correspond to the mean value SWAN output and observation data, respectively. The last one is M which represents the number of data points. Both bias and RMSE are expressed in meters.

3. Result and Discussion

SWAN verification. To assess SWAN performance in wave simulation, SWH from three buoys near the path of TC Kimi were analyzed (Fig. 2). Fig. 3 demonstrates a strong correlation between the observed data and SWAN output, particularly at Townsville and Emu Park. In Albatross Bay, SWH from SWAN seems to underestimate the observation data. In comparison, SWAN output in Townsville generally overestimates observation data. Different pattern spotted in Emu Park, where the SWAN output overestimates the lower wave heights while underestimating the higher wave heights.

To offer a more detailed comparison of SWH between SWAN output and observational data, bias, RMSE, and correlation coefficients were computed. The bias recorded in Albatross Bay is -0.11 m and meanwhile the RMSE is 0.14 m. This apparent in Fig. 3, where the SWH plot from SWAN and the observations display minimal discrepancies. Bias and RMSE in Albatross Bay are lower probably due to the wave in this location tends shorter compared to others. The best correlation value was noted at Emu Park, with a correlation coefficient of 0.95. As shown in Fig. 3, the SWAN output spreads near the reference line. Based on the statistical calculation, the results are confident enough to be used to perform wave simulation. Compared to Subasita 2018 [25], the study shows bias varies from -1.1 to 0.11 m, RMSE varies from 0.3 to 1.17 and Correlation varies from 0.66 to 0.75. Other study by Liang et al. [26] shows bias varies from -0.14 to 0.26 m, and RMSE varies from 0.36 to 0.64.

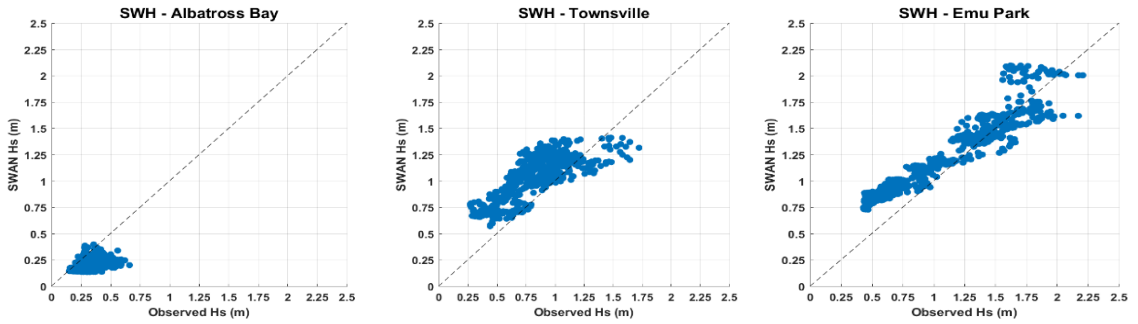

Figure 3. Scatter plots of SWH comparisons in 3 buoys.

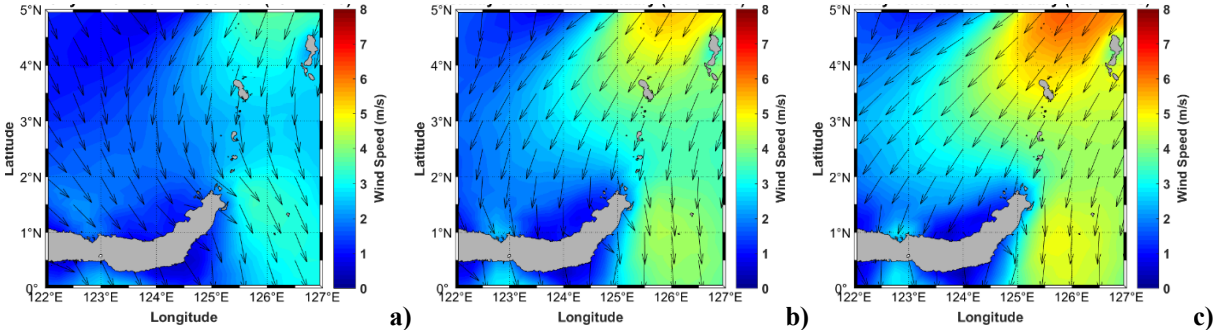

Figure 4. Wind climate in North Sulawesi during (a) December, (b) January, and (c) February period between 1974-2023.

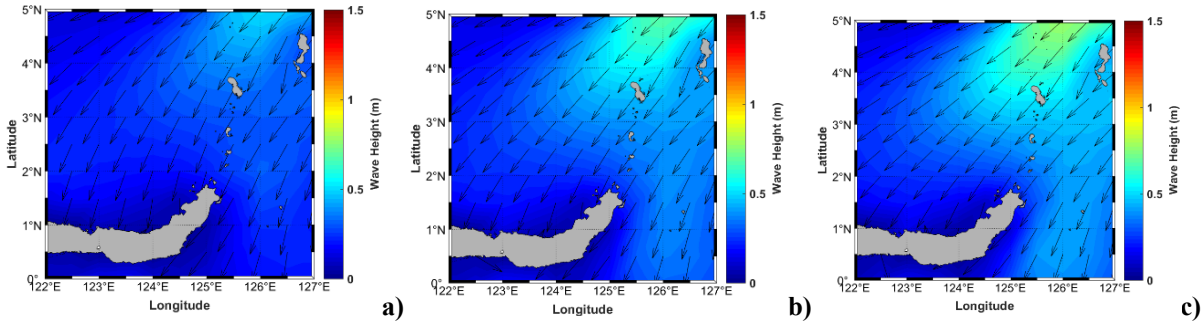

Figure 5. Wave climate in North Sulawesi during (a) December, (b) January, and (c) February period between 1974-2023.

Table 1. Statistical calculation in 3 buoys.

	Bias (m)	RMSE (m)	Correlation
Albatross Bay	-0.11	0.14	0.54
Townsville	0.21	0.27	0.80
Emu Park	0.15	0.23	0.95

Wave climate in DJF period in North Sulawesi. TC Kimi occurred in 15th to 19th of January 2021, so in this study we focused the wind and wave climate only on the DJF period. The DJF period marks the active phase of the Asian monsoon, with winds blowing from the Asian continent, passing through the Indonesian archipelago, and heading towards Australia. In North Sulawesi during DJF (Figure 4 and 5), the winds blow from the northwest-northeast, influenced by winds from the Pacific Ocean. In December, the highest wind speeds occur in the waters of the Sangihe and Talaud Islands and the Maluku Sea, ranging from 2.5 to 3.5 m/s. In January, the area of highest wind speeds expands to the eastern part of the Sulawesi Sea, with speeds between 3 and 5 m/s. During this period, wind speeds peak in February, reaching between 3 and 6 m/s, and extend to the central part of the Sulawesi Sea. During the DJF period, the wave direction follows the wind direction, moving towards the southwest. In December, the highest wave heights range between 0.25 to 0.5 meters, mainly in the waters around the Sangihe and Talaud Islands. By January, wave heights increase to between 0.25 and 0.75 meters, spreading into the Maluku Sea. In February, the waves reach their peak heights of 0.25 to 1 meter, extending into the Sulawesi Sea. This result confirms the previous study by Kurniawan et al. 2011 [35] and Ramdhani 2015 [36] where the wind and wave come from north-northeast during DJF period due to influence of Asian monsoon.

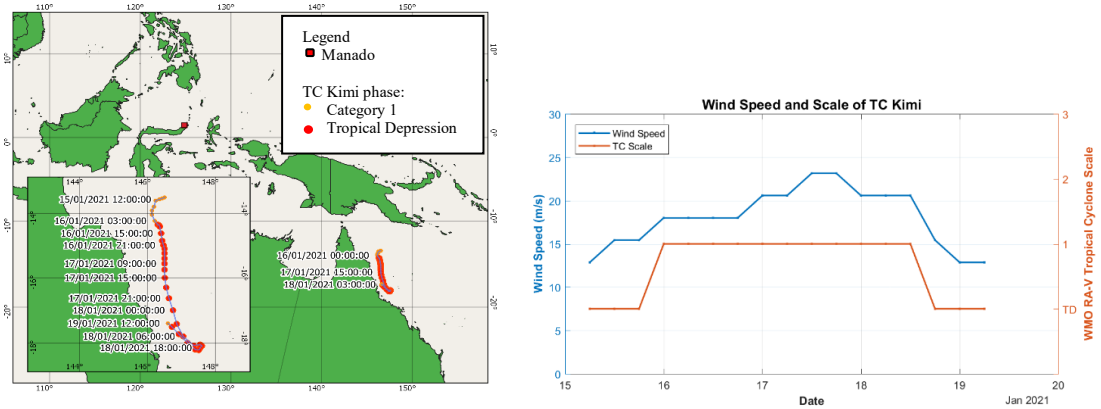

Figure 6. Location and trajectory (left), and intensity and the highest wind speed of TC Kimi (right).

TC Kimi. TC Kimi was an active tropical cyclone in the Australian region, a basin known for significant tropical cyclone activity, with 12% of global tropical cyclones occurring there [4]. Figure 6 shows that TC Kimi was first classified as a Tropical Depression (TD) at 06 UTC on 15th of January 2021, at the coordinates 146.5° E and 13.5° S. The cyclone moved southward and intensified into a Category 1, according to Australian Tropical Cyclone category scale by WMO, 2023 [39], by 00 UTC on 16th of January 2021. TC Kimi reached its peak intensity with wind speeds of 23.1 m/s (45 knots) between 12 and 18 UTC on 17th of January 2021. The cyclone then began to weaken, indicated by a reduction in wind speed, and reverted to a TD at 18 UTC on 18th of January 2021, coinciding with a shift in its trajectory towards the northwest. TC Kimi was officially declared dissipated after 06 UTC on 19th of January 2021.

Wind and SWH in North Sulawesi. The wind and SWH conditions were analysed based on the different phases of TC Kimi: before the formation of TC Kimi, peak intensity, and after TC Kimi dissipated. The phase before TC Kimi was selected at 00 UTC on 15th of January 2021, the peak intensity phase was at 12 UTC on 17th of January and the phase after TC Kimi dissipated was at 12 UTC on 19th of January. These time periods were selected to analyse the impact of TC Kimi activity towards wind and wave dynamics in North Sulawesi.

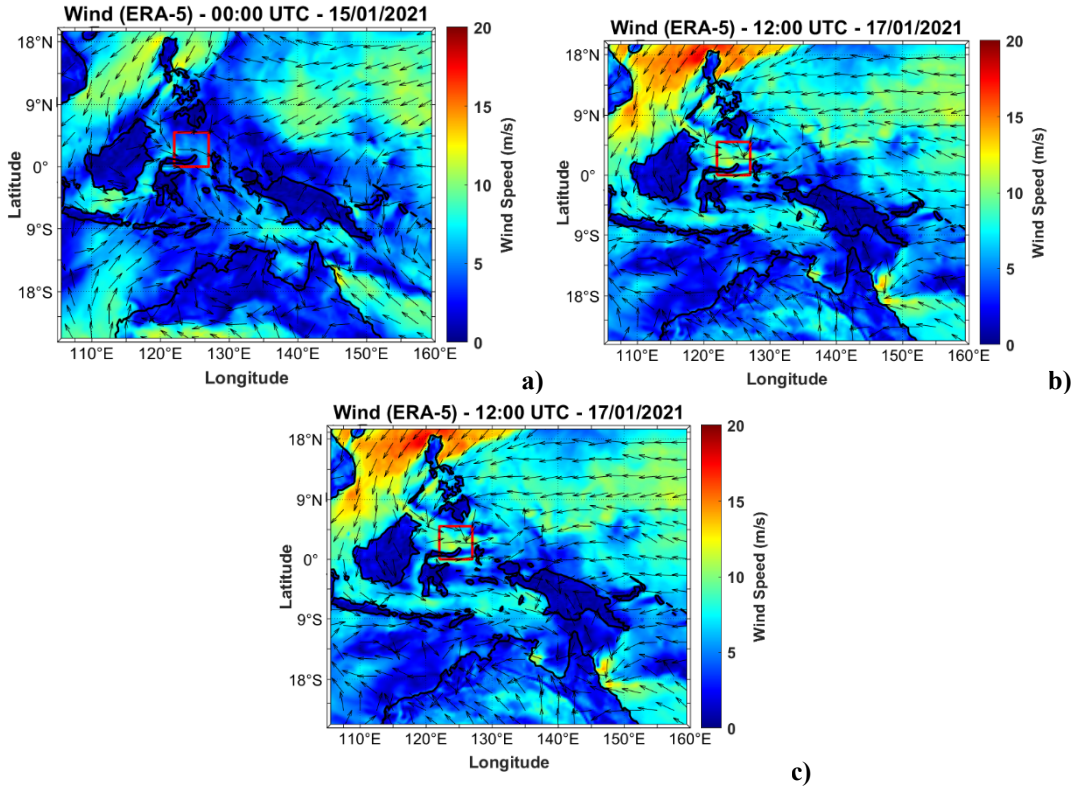

Figure 7. Wind speed and direction (a) pre-TC Kimi, (b) at the peak intensity and (c) post-TC Kimi. Red square shows the area of interest and red star (b) indicates the location of TC Kimi.

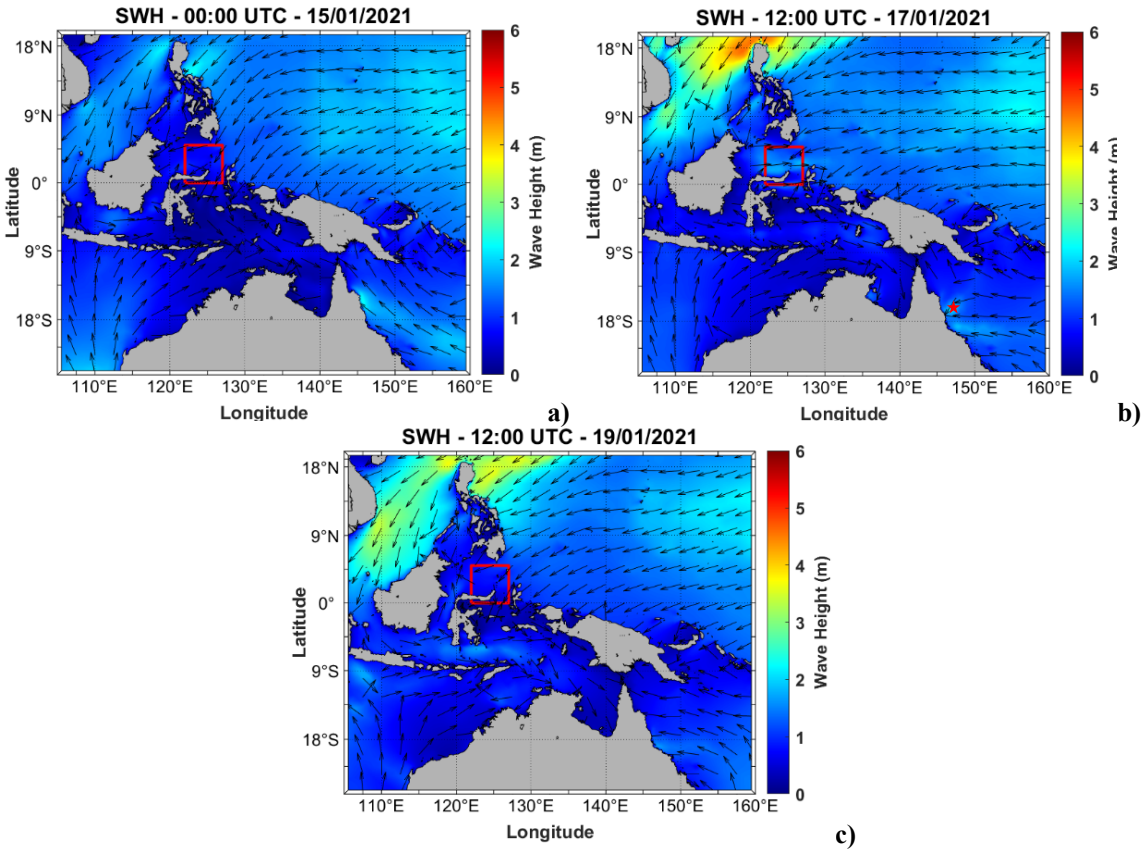

Figure 8. Wave height and direction before pre-TC Kimi, during the peak intensity and post-TC Kimi dissipated. Red square shows the area of interest and red star (b) indicates the location of TC Kimi.

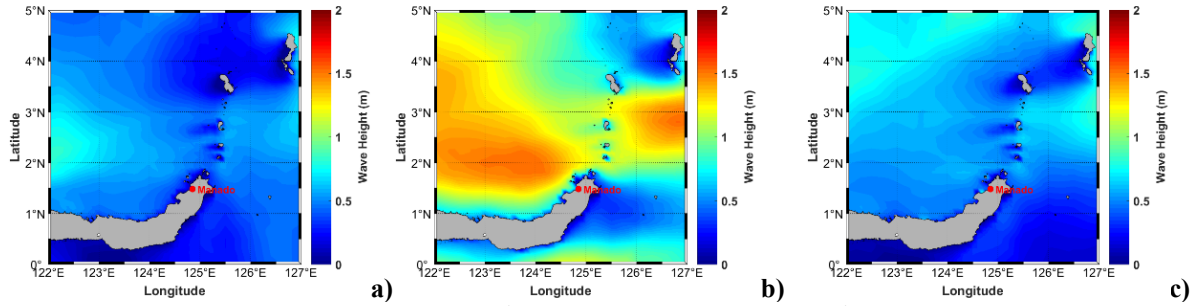

Figure 9. SWH anomaly at (a) 00 UTC on 15th of January, (b) 12 UTC on 17th of January, and (c) 12 UTC on 19th of January 2021

Before TC Kimi became active (Fig. 7a and 8a), the wind predominantly blew from the west-northwest at speeds ranging from 3-9 m/s. SWH were between 0.3-1 m and the direction looks irregular due to wave that comes from the Pacific Ocean meets the wave that formed in the western part of the Sulawesi Sea. At the strongest intensity (Fig. 7b and 8b), wind speed increased to 5-11 m/s and wind directions were from west-north. SWH also increased to 1-1.8 m. In the Maluku Sea, SWH were lower due to a shadow zone, in terms of the wind direction. Stronger wind speed also leads to the shifting of location where wave from Pacific Ocean meets the wave from Sulawesi Sea, which in this phase, the wave meets in the waters between Sangihe and Talaud. After TC Kimi dissipated (Fig. 7c and 8c), wind speed dropped to 3-5 m/s and the direction becomes irregular meanwhile the SWH also dropped to 0.5-1 m and the direction changes into its climatology (Fig. 5)

SWH anomaly (Fig. 9) are calculated from the difference of SWH in Fig. 7 and its climatological condition (Fig. 5), so that the change that occurred during TC Kimi active can be detected. Before TC Kimi active, SWH anomaly are between 0.4-0.7 m. The highest values are mainly in the western and eastern part, due to the wave climate in both areas are lower. In the northeastern part, the anomaly was low because of the wave climate in this area is higher compared to other area so the change is lower. At the strongest intensity of TC Kimi, SWH anomaly increased to between 0.4-1.3 m with the highest anomaly are mainly in the Sulawesi Sea and the northern part of Maluku Sea. This condition occurred

due to the high SWH at the strongest of TC Kimi occurred in those areas. Low SWH anomaly in the central Maluku Sea and Talaud waters are because of both areas are the shadow zone, relative to its direction (Fig. 8b). After TC Kimi dissipated, the SWH anomaly are decreased. High anomaly during this phase occurred in the northern area and east area because of the SWH are high in those areas, meanwhile the lowest anomaly is in the shadow areas.

Time lag calculations were performed to determine the delay in TC Kimi's impact on atmospheric dynamics in North Sulawesi. This analysis is crucial because TC Kimi and Sulawesi are located in different hemispheres (Fig. 2). The calculations were conducted for wind speed parameters in both regions. Additionally, SWH values at near Manado Bay were included to assess changes over time.

Before TC Kimi formed, there was an observed increase in wind speed in the TC Kimi area, consistently remaining above 6 m/s until the cyclone weakened. This increase in wind speed was followed by a rise in wind speed in North Sulawesi after a delay. Wind speeds in North Sulawesi increased several hours later, peaking on of 17th January 2021. After the wind speed in North Sulawesi rose, the SWH in the region also increased shortly thereafter and reaches 0.8 m. As TC Kimi began to weaken, wind speeds in both the TC Kimi area and North Sulawesi, as well as SWH in North Sulawesi, decreased. TC Kimi wind decreased mainly due the asymmetric distribution of wind speed that occurred during a TC. Usually, area behind the TC tends to have slower wind speed compared to the front area of a TC, relative to TC trajectory. This asymmetric wind speed distribution can occur due to various factors such as the forward speed of tropical cyclone systems, friction with the boundary layer, blocking action, beta effect and landfall [40]. After TC Kimi dissipated on 20th of January wind speeds in the TC Kimi area increased again, but wind speeds in North Sulawesi showed only a slight increase which indicates that in this period wind in TC Kimi have no impact on wind in North Sulawesi. This observation suggests that wind in the TC Kimi area has a moderate correlation with wind speed changes in North Sulawesi.

To determine the time lag, it is necessary to calculate the correlation for each hourly lag and plot the results on a cross-correlogram. Fig. 12 shows the highest correlation occurs at a time lag of +19 hours, with a correlation value of 0.49. This suggests a moderate correlation between wind speed in the TC Kimi area and wind speed in North Sulawesi. The +19-hour time lag indicates that it takes 19 hours for the wind speed in the TC Kimi area to impact the wind speed in North Sulawesi.

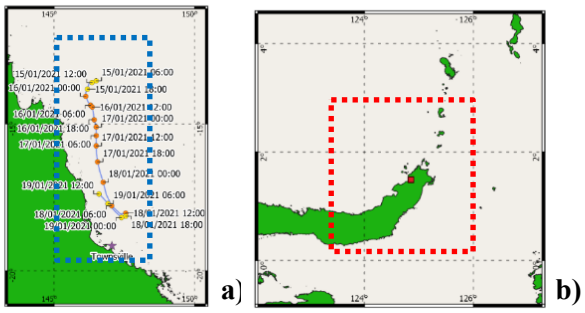

Figure 10. Dashed boxes show locations to calculate the spatial average in (a) TC Kimi and (b) North Sulawesi.

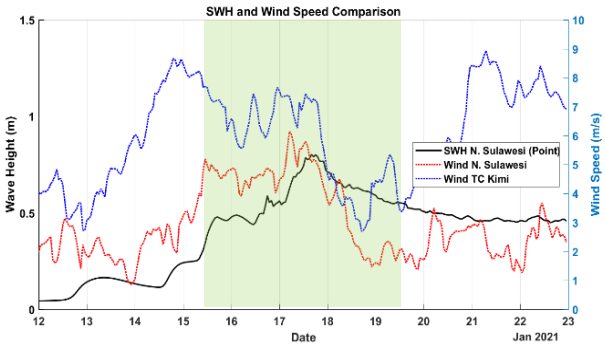

Figure 11. Wind data of TC Kimi (blue), North Sulawesi (red) and SWH of North Sulawesi (black). Green shade represents the time of TC Kimi was active.

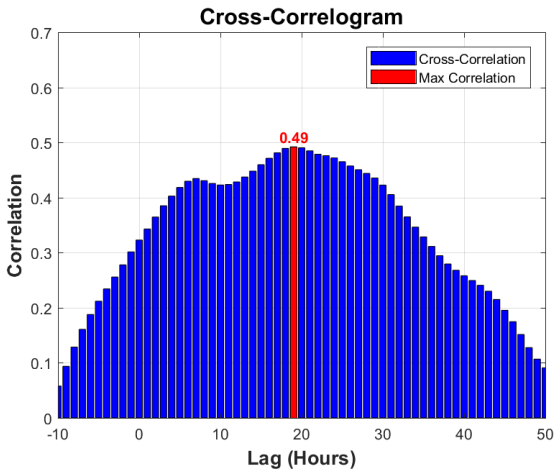

Figure 12. Cross-correlogram of wind speed of TC Kimi and wind speed in N. Sulawesi.

4. Conclusion

During the DJF period, winds blow from the northwest to the northeast, while waves move toward the southwest. This indicates that the winds in North Sulawesi are strongly influenced by the monsoon, whereas the waves are primarily driven by those coming from the Pacific. During the peak intensity of TC Kimi, SWH showed a significant increase compared to before TC active and after TC Kimi dissipated, which the SWH reach 1.8 m in the

Sulawesi Sea and Maluku Sea. The high significant wave height (SWH) was influenced by several factors, including strong wind speeds, the vast area of the Sulawesi Sea, which allows for a long fetch, and the westward wind direction that optimally utilizes the fetch in the region. The high SWH during the peak of TC Kimi leads to the high anomaly compared to the climatological conditions reaching 0.4-1.3 meters. This increase triggered by a significant rise in SWH at TC Kimi's peak intensity. Influence of TC Kimi to the wind speed has a time lag of approximately 19 hours.

Acknowledgement

We sincerely appreciate for technical support from the Indonesian Meteorological, Climatological, and Geophysical Agency (BMKG). This study is greatly helped by their valuable resources and expertise.

References

[1] E. Yulihastin, A. Taofiqurohman, I. Fathrio, et al, "Evolution of double vortices induce tropical cyclogenesis of Seroja over Flores, Indonesia," *Nat Hazards* vol. 117, 2675–2692, 2023. https://doi.org/10.1007/s11069-023-05961-8

[2] M.F.A. Ismail, J. Karstensen, J. Ribbe, et al, "Seasonal mixed layer temperature and salt balances in the Banda Sea observed by an Argo float," *Geosci. Lett. 10*, vol. 10, 2023. https://doi.org/10.1186/s40562-023-00266-x

[3] D. Yuan, X. Yin, X. Li, et al, "A Maluku Sea intermediate western boundary current connecting Pacific Ocean circulation to the Indonesian Throughflow," *Nat Commun* 13, 2093, 2022. https://doi.org/10.1038/s41467-022-29617-6

[4] H. Ramsay, "The Global Climatology of Tropical Cyclones" Oxford Research Encyclopedia of Natural Hazard Science. Retrieved 19 May. 2023.

[5] N.S. Ningsih, A. Azhari, and T. M. Al-Khan, "Wave climate characteristics and effects of tropical cyclones on high wave occurences in Indonesian waters: Strengthening Sea transportation safety management," *Ocean and Coastal Management* vol. 243, 106738, Jul. 2023, doi.org/10.1016/j.ocecoaman.2023.106738.

[6] H. Yang, B. Liang, and Z. Shao, "Study on the range of tropical cyclones on ocean waves," *Ocean Engineering*, vol. 266, Oct. 2022, doi.org/10.1016/j.oceaneng.2022.112864.

[7] H. Woo and K. Park, "Estimation of Extreme Significant Wave Height in the Northwest Pacific Using Satellite Altimeter Data Focused on Typhoons (1992–2016)," *Remote Sens.* vol. 13 no. 6, 2021, doi.org/10.3390/rs13061063.

[8] F. Ardhuin, B. Chapron, and F. Collard, "Observation of swell dissipation across oceans," *Geophys. Res. Lett.*, vol. 36, L06607, 2009, doi:10.1029/2008GL037030.

[9] Y. Hu, W. Shao, Y. Wei, and J. Zuo, "Analysis of Typhoon-Induced Waves along Typhoon Tracks in the Western North Pacific Ocean, 1998–2017," *J. Mar. Sci. Eng.* Vol. 8, 521. 2020, doi:10.3390/jmse8070521

[10] World Meteorological Organization, "Guide to wave analysis and forecasting", Geneva, ISBN 978-92-63-10702-2, 2018.

[11] H. Hritz, and A. F. Franzidis, "Exploring the economic significance of the surf tourism market by experience level" *Journal of Destination Marketing & Management*, vol. 7, pp. 164-169, Oct. 2016, doi.org/10.1016/j.jdmm.2016.09.009.

[12] A. N. Effendi, M. F. Geonova, P. Widodo, H. J. R. Saragih, P. Suwarno, D. A. Mamahit, and Trismadi, "Karakteristik gelombang laut Indonesia untuk mendukung kegiatan laut dan keamanan maritim", vol. 7, no. 2, Apr. 2023, doi.org/10.33379/gtech.v7i2.1989.

[13] R. D. Aror, W. Patty, and A. Ramdhani, "Utilization of Wavewatch-III model output data for high wave analysis". *Indonesian Journal of Marine Sciences*, Vol. 24 No.3, pp. 132-138, Sept. 2019. doi.org/ 10.14710/ik.ijms.24.3.132-138

[14] H. Burrahman, "Analysis of Oceanographic and Atmospheric Parameters During Inundation in Manado (Case Study 15-17 January 2021)", Proceeding for *National Seminar of Physics and Applications*, 2021, E-ISSN: 2548-8325 / P-ISSN 2548-8317.

[15] N. Booij, C. R. Ris and L. H. Holthuijsen, "A third generation wave model for coastal regions: 1. Model description and validation" *Journal of Geophysical Research*, vol. 104 no. 4. pp. 7649-7666, 1999.

[16] SWAN Team, "SWAN Manual", 2003.

[17] Y. Jiang, Z. Rong, P. Li, T. Qin, X. Yu, Y. Chi, and Z. Gao, "Modelling waves over the Changjiang River Estuary using a high-resolution unstructured SWAN model," *Ocean Modelling*, vol. 173, 2022.

[18] R. Rachmayani, N. S. Ningsih, S. R. Adiprabowo, and S. Nurfitri, "Ocean wave characteristic in the Sunda Strait using Wave Spectrum Model", *IOP Conf. Ser.: Earth Environ. Sci.* 139 012025, 2018.

[19] A. Wurjanto, and J. A. Mukhti, "Sensitivity analysis for wind-driven significantwave height model in SWAN: A Sunda Strait case". *IOP Conf. Ser.: Earth Environ. Sci.* 729 012035, 2021.

[20] M. Zijlema, "Computation of wind-wave spectra in coastal waters with SWAN on unstructured grids" *Coastal Engineering*, vol. 57, pp. 267-277, 2010.

[21] G. Napitupulu, M. F. Nuruddin, N. A. Fekranie, and I. Magdalena, "Analysis of wind generated wave characteristics by SWAN model in Balikpapan Bay", *IOP Conf. Ser.: Earth Environ. Sci.* 930 012067, 2021.

[22] R. Rachmayani, N.S. Ningsih, and I. Ardiansyah, "The effect of reclamation on the significant wave height changes in Jakarta Bay during Hagibis and Mitag typhoons", *Journal of Ocean Engineering and Marine Energy*, vol. 9, pp. 165-179, 2022, doi.org/10.1007/s40722-022-00249-8.

[23] M. Mao, A. J. van der Westhuysen, M. Xia, D. J. Schwab, and A. Chawla, "Modeling wind waves from deep to shallow waters in Lake Michigan using unstructured SWAN", *Journal of Geophysical Research: Oceans*, vol. 121, pp. 3836-3865, Jun. 2016. doi.org/ 10.1002/2015JC011340.

[24] J. Lu, J. Shi, W. Zhang, J. Xia, and Q. Wang, "Numerical simulations on waves in the Northwest Pacific Ocean based on SWAN models," *J. Phys.: Conf. Ser.* 2486 012034, 2023.

[25] N. Subasita, "Influence of tropical cyclones on the statistical properties of extreme waves in the tropical Indian Ocean," Thesis Program Magister, Utrecht University, 2018.

[26] B. Liang, H. Gao, Z. Shao," Characteristics of global waves based on the third-generation wave model SWAN," *Marine Structures*, vol. 64, pp. 35-53, Oct. 2018.

[27] G. J. Komen, L. Cavaleri, M. Donelan, K. Hasselmann, S. Hasselmann and P. A. E. M. Janssen, "Dynamics and Modelling of Ocean Waves," Cambridge, Cambridge, University Press, 1994.

[28] L. H. Holthuijsen, "Waves in the Ocean and Coastal Waters," Cambridge: Cambridge University Press. ISBN-13 978-0-511-27021-5, 2007.

[29] Copernicus Climate Change Service (2023): ERA5 hourly data on single levels from 1940 to present. Copernicus Climate Change Service (C3S) Climate Data Store (CDS), DOI: 10.24381/cds.adbb2d47 (Accessed on 15-MAR-2024).

[30] K. Amarouche, A. Akpinar, A. Rybalko, and S. Myslenkov, "Assessment of SWAN and WAVEWATCH-III models regarding the directional wave spectra estimates based on Eastern Black Sea measurements," *Ocean Engineering* vol. 272 113944, Feb. 2023, doi.org/10.1016/j.oceaneng.2023.113944.

[31] E. Çalısır, M.B. Soran, A. Akpınar, "Quality of the ERA5 and CFSR winds and their contribution to wave modelling performance in a semi-closed sea". *J. Oper. Oceanogr.* doi.org/10.1080/1755876X.2021.1911126, 2021.

[32] Soran, M.B., Amarouche, K., Akpınar, A., 2022. Spatial calibration of WAVEWATCH III model against satellite observations using different input and dissipation parameterizations in the Black Sea. Ocean Eng. 257, 111627 doi.org/10.1016/J.OCEANENG.2022.111627.

[33] Gebco gridded global bathymetry data. British Oceanographic Data Centre, Liverpool, United Kingdom, 2024.

[34] A. Semedo, K. Suselj, A. Rutgersson, A. Sterl, "A global view on the wind sea and swell climate and variability from ERA-40," *Journal of Climate*, vol. 24, no. 5, pp. 1461-1479, 2011, doi.org/10.1175/2010JCLI3718.1.

[35] R. Kurniawan, M. N. Habibie, and Suratno, "Variasi bulanan gelombang laut di Indonesia Monthly variation of wave height in Indonesia," *Jurnal Meteorologi dan Geofisika*, vol. 12, no.3, 2011.

[36] A. Ramdhani, "The Effect of Tropical Cyclones and Madden Julian Oscillation (MJO) on HighWave Events Using the Wavewatch III Model in Inner Seas of Indonesia". Ph.D. Thesis, Institut Teknologi Bandung, Bandung, Indonesia, 2015.

[37] E. Pallares, J. Lopez, M. Espino and A. Sanchez-Arcilla, "Comparison between nested grids and unstructured grids for a high-resolution wave forecasting system in the western Mediterranean Sea," *Journal of Operational Oceanography*, vo. 10, no. 1, 45-58. 2017, dx.doi.org/10.1080/ 1755876X.2016.1260389.

[38] K.J. Roberts, W.J. Pringle, and J.J. Westerink, "OceanMesh2D 1.0: MATLAB-based software for two-dimensional unstructured mesh generation in coastal ocean modelling," *Geosci. Model Dev. (GMD)* vol. 12, pp. 1847–1868. doi.org/10.5194/gmd-12-1847-2019.

[39] World Meteorological Organization, "Regional Association V - Tropical Cyclone Operational Plan for the South Pacific and South-East Indian Ocean," Geneva, 2023.

[40] M. Olfateh, D. P. Callaghan, P. Nielsen, and T. E. Baldock, "Tropical cyclone wind field asymmetry—Development and evaluation of a new parametric model," J. Geophys. Res. Oceans, 122, 458–469, 2007, doi:10.1002/2016JC012237.